Target fragment energies and momenta in the reaction of 4.8 GeV ^{12}C and 5.0 GeV ^{20}Ne with ^{238}U

W. Loveland and Cheng Luo*
Department of Chemistry, Oregon State University, Corvallis, Oregon 97551

P. L. McGaughey, D. J. Morrissey, and G. T. Seaborg
Nuclear Science Division, Lawrence Berkeley Laboratory and Department of Chemistry, University of California, Berkeley, California 94720
(Received 14 October 1980)

Target fragment recoil properties were measured using the thick-target–thick-catcher technique for the interaction of 4.8 GeV ^{12}C and 5.0 GeV ^{20}Ne with ^{238}U. The target fragment energies and momenta are very similar for the reaction of 4.8 GeV (400 MeV/nucleon) ^{12}C and 5.0 GeV (250 MeV/nucleon) ^{20}Ne with ^{238}U. In the complex variation of fragment momenta with their N/Z ratio, one finds evidence suggesting the existence of several mechanisms leading to the formation of the target fragments. Comparison of these results with the predictions of the intranuclear cascade model of Yariv and Fraenkel and the firestreak model shows that both model predictions grossly overestimate the target fragment momenta.

[NUCLEAR REACTIONS ^{238}U(^{12}C,x), E=4.8 GeV; ^{238}U(^{20}Ne,x), E=5.0 GeV; measured target fragment recoil properties; deduced target fragment energies, momenta; relativistic heavy ion reactions; target fragmentation; spallation; fission; intranuclear cascade model; firestreak model; thick-target–thick-catcher technique; Ge(Li) gamma-ray spectroscopy.]

I. INTRODUCTION

The study of the fragmentation of a ^{238}U target nucleus induced by relativistic heavy ion (RHI) projectiles has from the outset revealed many new and interesting phenomena. In the first measurements of the yields of target fragments of differing Z and A from the reaction of 25.2 GeV ^{12}C with ^{238}U, Loveland *et al.*[1] found, in addition to the expected yields of fission fragments, surprisingly large yields of fragments with $160 \leq A \leq 190$ (see Fig. 1). Subsequent measurements by McGaughey *et al.*[2] for the reaction of 8.0 GeV ^{20}Ne with ^{238}U showed a smaller enhancement of these heavy product yields (see Fig. 1), but the yields of these products still appeared to exceed any such yields observed in the reaction of protons with ^{238}U. Spurred by these observations, Jacak and coworkers[3] extended the previous measurements[4,5] of target fragment yields in the reaction of 28 GeV protons with ^{238}U beyond mass number 160 to see if any evidence could be found for such yields in proton-induced reactions. A small group of significant product yields were found for $185 \leq A \leq 200$ (see Fig. 1). Comparison of the experimental yield distributions with the yield distributions calculated using the abrasion-ablation model,[6] the intranuclear cascade model of Yariv and Fraenkel,[7] and the firestreak model[8] demonstrated that these fragments could be understood as being the survivors of a deep spallation process (involving significant projectile-target overlap) that resulted in the removal of as many as 80 nucleons from the target nucleus. These studies of target fragmentation involving ^{238}U target nuclei appear to show features, [i.e., the variation of yield distributions with projectile energy (violation of "limiting fragmentation") and the general nonequivalence of product distributions from RHI- and proton-induced reactions (violation of "factorization")] not seen in the interaction of RHI's with lighter targets[9-11] [Small deviations from limiting fragmentation and factorization were observed for light products from the

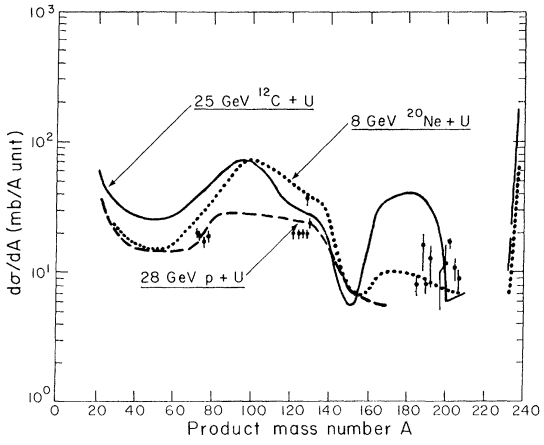

FIG. 1. Isobaric yields of fragments produced in the interaction of relativistic projectiles with uranium. The data points are the measurements of Jacak *et al.* (Ref. 3) for the reaction of 28 GeV protons with uranium.

reaction of 25.2 GeV ^{12}C with Cu (Ref. 12) and Ag.[13]]

One of the most interesting questions to be addressed in the study of target fragmentation in relativistic nucleus-nucleus collisions is the mechanism(s) of energy transfer between projectile and target. Do the nucleons in the projectile and target interact as individual particles or is there a collective character to the interaction? At what value, if any, of the transferred energy does "saturation" take place? These and many similar questions are important components of the attempt to use relativistic nucleus-nucleus collisions to create new and unusual conditions in nuclear matter such as shock waves or to use these reactions to produce new nuclear species. The most sensitive experimental method for studying this transfer is to measure the target fragment kinematic properties (i.e., their energies, momenta, and angular distributions). In support of this idea, we note that in the reaction of 8.0 GeV ^{20}Ne with Ta, a consortium of investigators from ANL, BNL, and LBL/OSU found[14] that the target fragment kinematic properties differed from those observed in the reaction of 25 GeV ^{12}C or relativistic protons with heavy targets despite the fact that limiting fragmentation with respect to product yields was observed.[11] The measurement of target fragment momenta and energies can be more indicative of primary reaction processes than the measurement of target fragment yields because in the former measurements the effect of primary reaction processes and secondary processes involving deexcitation of the excited primary fragments can be unraveled.[15]

In this paper, we report the results of measurements of target fragment kinematic properties, using the thick-target–thick-catcher technique, for the reaction of 4.8 GeV (0.4 GeV/nucleon) ^{12}C and 5.0 GeV (0.250 GeV/nucleon) ^{20}Ne with ^{238}U. In Sec. II, we discuss the experimental measurements and their analysis in terms of the two-step vector model of high energy reactions, while in Sec. III we discuss the results in detail comparing them to results of studies of relativistic proton-uranium collisions and current models of RHI reactions. In Sec. IV, we summarize the conclusion of our study.

II. EXPERIMENTAL

Beams of 4.8 GeV ^{12}C and 5.0 GeV ^{20}Ne from the LBL Bevalac were used to irradiate a single thick depleted U foil (<400 ppm ^{235}U) of thickness 56.1 and 51.3 mg/cm^2, respectively, surrounded by Mylar catcher foils of thickness 36 mg/cm^2. The total particle fluences and irradiation lengths were 6.19×10^{13} ^{12}C/821.4 min and 1.00×10^{13} ^{20}Ne/639.8 min, respectively. Assay of the radioactivities of the target fragments that stopped in the target, the forward, and the backward catcher foils by γ-ray spectroscopy began approximately one hour after the end of irradiation and measurements continued for approximately six weeks. Standard techniques which have been described elsewhere[16] were used to identify the radionuclides present in each sample and to determine the activity of each nuclide in the forward, backward, and target foils. No corrections were made to any of the activities for the effect of secondary induced reactions because previous studies[17] of $p+U$ collisions using recoil techniques and targets five times thicker than those used in this work revealed such corrections to be <5%. (The thicker targets used in the proton induced reaction studies should approximately compensate for the higher charged particle multiplicities observed in the RHI-induced reactions.)

The results of these measurements are presented as the fractions of each radionuclide which recoiled out of a target of thickness W (mg/cm^2) in the forward and backward directions denoted by F and B, respectively. Tables I and II give a tabulation of the results for the forward-to-backward ratio F/B and a quantity approximately equal to the mean range of the recoil in the target material, $2W(F+B)$, for the two reactions studied. Because of the complex variation of these quantities with the N/Z of the fragment, a simple plot of F/B or $2W(F+B)$ vs A would be a confusing jumble. Therefore we have chosen a set of common nuclides for both data sets (indicated by the symbol * in Table I) and have plotted the A dependence of the ratio of F/B and $2W(F+B)$ measured in one reaction to that measured in the other reaction in Fig. 2. In Fig. 3 we plot the ratios of the F/B and $2W(F+B)$ values obtained for the 4.8 GeV $^{12}C+^{238}U$ reaction to similar values for common nuclides for the reaction of 450 MeV protons[17,18] and 3 GeV protons[18-22] with ^{238}U. The full complexity of the F/B values is shown in Fig. 4 for the 4.8 GeV $^{12}C+^{238}U$ reaction.

The results were transformed into kinematic quantities using the two step vector model of high energy nuclear reactions, developed by Sugarman and co-workers.[23,24] The equations used in the analysis have been recently described by Winsberg.[25] In this model, the velocity $\vec{V}_l$ of a recoil nuclide in the laboratory system is taken to be the sum of two vectors $\vec{V}_l=\vec{v}+\vec{V}$. The velocity vector $\vec{v}$ results from the initial fast projectile-target interaction (the "abrasion" step of the abrasion-ablation model) while the velocity vector $\vec{V}$, assumed to be isotropic in the moving system, results from the slow deexcitation of the excited primary fragment (the "ablation step"). The vector

TABLE I. Target fragment recoil properties of 4.8 GeV $^{12}C+^{238}U$. * indicates a nuclide was observed in both 4.8 GeV $^{12}C+^{238}U$ and 5.0 GeV $^{20}Ne+^{238}U$.

Nuclide	E_γ (keV)	F/B	$2W(F+B)$	Nuclide	E_γ (keV)	F/B	$2W(F+B)$
*^{24}Na	1368.6	5.5±0.8	20.3±2.6	^{90}Y^m	202.4	1.7±0.3	8.0±0.9
*^{28}Mg	400.6	4.6±1.0	18.3±2.9	^{90}Nb	1129.1	2.6±0.6	5.6±0.9
	941.7			^{91}Sr	555.6	1.3±0.2	11.0±1.4
	1342.2				652.9		
	1778.9				749.8		
*^{43}K	372.0	4.7±1.0	14.6±3.0		925.8		
	396.0				1024.3		
	593.5			^{92}Y	934.5	1.2±0.3	7.9±1.5
^{44}Sc^m	270.9	3.2±0.4	10.9±1.0	^{93}Mo^m	684.6	2.0±1.8	5.8±1.8
	1157.0				1477.2		
^{46}Sc	889.3	3.5±0.9	13.0±1.6	^{95}Zr	724.2	1.1±0.1	9.6±0.7
	1120.5				756.7		
*^{48}Sc	983.5	2.9±0.5	10.0±1.2	^{95}Nb	765.8	1.5±0.3	4.2±0.5
	1037.6						
	1312.1			^{95}Tc	765.8	3.3±0.8	6.2±0.8
^{48}V	983.5	3.4±0.5	11.4±1.0	*^{96}Nb	460.0	1.3±0.3	7.6±1.1
	1311.6				568.9		
^{56}Mn	846.6	2.7±0.9	8.3±2.1		849.9		
					1091.3		
^{59}Fe	1099.2	2.3±1.3	8.8±1.6		1200.2		
	1291.6				1497.7		
^{69}Zn^m	438.7	1.8±0.2	11.0±1.1	*^{96}Tc	812.5	2.2±0.3	6.5±0.6
^{71}As	174.9	2.6±0.4	9.5±1.4		849.9		
					1126.8		
*^{72}As	834.0	1.6±0.2	9.6±0.8	^{97}Ru	215.7	2.5±0.6	5.4±0.5
^{74}As	595.9	2.1±0.3	9.4±1.3	*^{97}Zr	355.4	1.2±0.2	9.8±2.0
*^{76}As	559.1	2.2±0.3	8.1±0.8		743.4		
					1148.0		
^{77}Br	520.7	2.1±1.2	7.9±4.5		1750.5		
	579.4						
				*^{99}Mo	140.5	1.3±0.1	9.6±0.2
^{78}As	694.9	1.8±0.9	14.1±9.5		181.1		
					364.5		
^{81}Rb	190.4	2.4±0.4	9.3±3.6		739.6		
^{82}Br	554.3	1.2±0.3	6.6±1.0				
	689.4			^{101}Rh^m	306.8	2.4±1.0	5.9±1.3
	827.8			^{103}Ru	497.1	1.4±0.2	9.3±0.9
	1043.9						
	1317.4			^{105}Ru	316.5	1.1±0.2	9.8±1.5
	1474.8				469.4		
					676.3		
^{82}Rb^m	698.4	2.1±0.7	6.7±2.3		724.2		
	827.6						
	1044.1			^{105}Rh	319.2	1.9±0.3	7.9±0.7
	1317.5						
				^{106}Ag^m	406.0	0.8±0.4	6.3±1.8
^{83}Rb	520.3	1.9±0.7	8.1±1.5		429.5		
					450.8		
^{86}Rb	1078.8	1.7±0.3	7.4±1.0		1199.1		
^{87}Y^m	381.1	2.2±0.2	6.1±1.0		1527.0		
^{88}Zr	392.8	2.7±0.7	6.3±1.0	^{111}In	150.6	2.5±0.3	5.2±1.9
					171.3		
^{88}Y	898.0	2.1±0.2	9.3±2.8		245.4		
	1836.1						
				^{111}Pd^m	172.1	1.5±0.4	10.7±2.2
*^{89}Zr	909.2	2.2±0.3	7.5±0.6				

TABLE I. (*Continued*).

Nuclide	E_γ (keV)	F/B	$2W(F+B)$	Nuclide	E_γ (keV)	F/B	$2W(F+B)$
^{115}Cd	492.3 527.9	1.3±0.4	9.4±1.9	^{132}I	667.7 954.6	1.3±0.3	5.3±0.8
^{115}In^m	336.3	1.3±0.6	13.5±6.8	*^{133}I	529.5	1.1±0.2	8.8±0.9
^{117}Sn^m	158.4	1.7±1.1	9.0±6.2	^{135}Xe	249.6	1.2±0.2	8.2±0.9
^{117}Sb	158.5	1.5±0.4	5.4±1.6	^{135}I	1038.8 1260.5 1458.1 1678.3 1791.5	1.4±0.3	8.7±1.1
^{119}Te^m	1136.0 1212.7	2.4±0.2	5.1±0.5				
^{120}Sb	197.3	1.7±0.2	4.5±0.6				
^{121}Te	573.1	2.8±0.5	4.1±0.7	^{136}Cs	176.7 340.6 818.5 1048.1 1235.4	1.1±0.1	7.0±1.7
^{122}Sb	563.9	1.4±0.3	8.1±1.1				
^{124}Sb	602.7 1691.0	0.8±0.3	6.9±2.0				
^{124}I	602.7 1691.0	1.8±0.4	6.5±0.8	^{139}Ce	165.8	1.5±0.3	2.4±0.2
				^{140}Ba	423.7 537.3	1.1±0.2	5.3±0.5
^{127}Sb	252.7 473.2 685.7	1.0±0.1	8.7±2.1	^{141}Ce	145.4	1.2±0.1	7.1±0.7
				^{145}Eu	893.7	2.4±0.4	2.3±0.2
^{130}I	448.0 739.4 1157.3	1.4±0.2	6.9±3.7	*^{146}Gd	747.4	5.5±1.5	1.8±0.3
				*^{149}Gd	149.7	4.3±0.6	2.7±0.3
^{131}Ba	123.7 216.0	2.6±0.3	4.4±0.3	^{151}Tb	287.2	10.7±3.5	1.9±0.4
				^{167}Tm	207.8	3.2±2.0	1.4±0.2
*^{131}I	364.5 637.0	1.2±0.1	8.4±4.5	^{169}Lu	960.3	3.2±2.0	2.4±1.2
^{132}Te	228.2 667.7 954.6 1398.5	1.1±0.1	7.1±0.6	^{185}Pt	197.5	1.2±1.0	1.2±1.0
				^{198}Au	411.8	2.1±0.7	3.7±1.0
				^{198}Tl	411.8	3.3±1.1	2.8±0.6
^{132}Cs	667.7	1.7±1.2	5.7±3.0	^{209}At	545.1	2.1±0.6	2.3±0.6

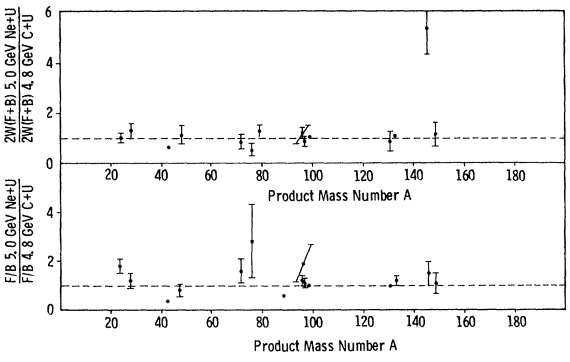

FIG. 2. Selected ratios of target fragment F/B and $2W(F+B)$ values for the reactions of 4.8 GeV ^{12}C and 5.0 GeV ^{20}Ne with ^{238}U.

$\vec{v}$ is assumed to be constant while the values of the vector $\vec{V}$ are assumed to have a Maxwellian distribution. No correlation is assumed to exist between the two vectors. The vector $\vec{v}$ can be decomposed into its two orthogonal components parallel and perpendicular to the beam ($v_{\parallel}$ and $v_{\perp}$). In this analysis we have assumed $v_{\perp}=0$. In converting product ranges into kinetic energies, we used the range-energy tables of Northcliffe and Schlling.[26] The results of this analysis are tabulated in Tables III and IV and are shown for the 4.8 GeV ^{12}C+^{238}U system in Fig. 5. The validity of using this analysis for RHI-induced reactions is discussed in Ref. 14.

III. DISCUSSION OF RESULTS

One question of continuing interest concerning the mechanism(s) of energy transfer in relativistic

TABLE II. Target fragment recoil properties of 5.0 GeV $^{20}Ne+^{238}U$.

Nuclide	F/B	$2W(F+B)$ (mg/cm^2)
^{24}Na	9.8±0.9	20.5±3.1
^{28}Mg	5.6±0.8	24.5±4.9
^{43}K	1.9±0.2	8.1±1.2
^{48}Sc	2.4±0.6	10.9±3.3
^{72}As	2.6±0.8	7.9±2.8
^{76}As	6.1±3.1	3.7±2.2
^{87}Y	2.1±0.2	7.5±1.1
^{89}Zr	1.4±0.2	8.8±1.8
^{96}Tc	2.6±0.4	8.0±1.0
^{96}Nb	2.5±0.8	8.8±3.5
^{97}Zr	1.3±0.1	7.9±0.8
^{99}Mo	1.3±0.1	9.5±0.5
^{131}I	1.2±0.1	6.6±1.0
^{133}I	1.3±0.1	8.7±0.9
^{146}Gd	8.0±2.0	9.7±1.0
^{149}Gd	4.6±1.4	3.0±1.2
^{160}Er	1.7±1.0	4.7±0.5

nucleus-nucleus collisions is the question of whether the energy transfer scales as the total projectile kinetic energy or as the energy per nucleon of the projectile. It is of interest in this regard to compare the target fragment kinematic properties for the reaction of 4.8 GeV ^{12}C and 5.0

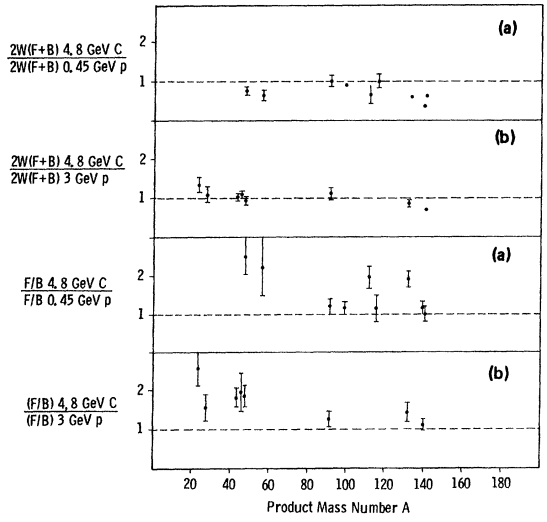

FIG. 3. Selected ratios of target fragment F/B and $2W(F+B)$ values for the reaction of 4.8 GeV ^{12}C to those measured for the reaction of (a) 450 MeV and (b) 3 GeV protons with ^{238}U.

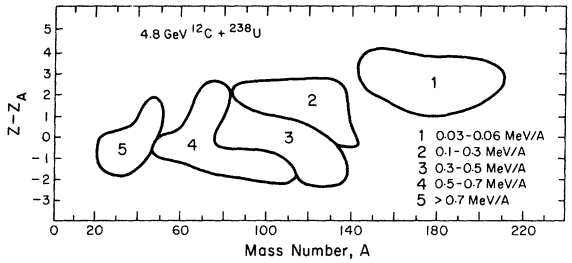

FIG. 4. A contour plot of the fragment F/B values as a function of the fragment mass number A and its position relative to the center of the valley of β stability ($Z-Z_A$) for the reaction of 4.8 GeV ^{12}C with ^{238}U.

GeV ^{20}Ne with ^{238}U (approximately equivalent total projectile kinetic energy, considerably different energy per nucleon). By examining the data in Fig. 2, one can see that, within experimental error, the target fragment kinematic properties for the two systems are generally similar with no obvious systematic differences between them. (In Fig. 2, 20 of the 30 common points agree within one standard deviation; 25 of 30 agree within two standard deviations.) While these experimental data are necessary but not sufficient observations for establishing the scaling of the energy transfer with total projectile kinetic energy, they probably do serve to justify the representation of the trends of both data sets by the discussion of the more complete, more precisely known data from the 4.8 GeV $^{12}C+^{238}U$ reaction. We shall adopt this viewpoint from this point forth. The observation of the equivalence of the two data sets is consistent with prior observations of Cumming *et al.*[9] and Loveland *et al.*[11] that the target fragment yields from RHI induced reactions most resemble the yields from reactions induced by protons of the same total projectile energy. This observation is also consistent with the data of Kaufman *et al.*[10] who found that the target fragment recoil properties from the reaction of 25.2 GeV ^{12}C with ^{197}Au

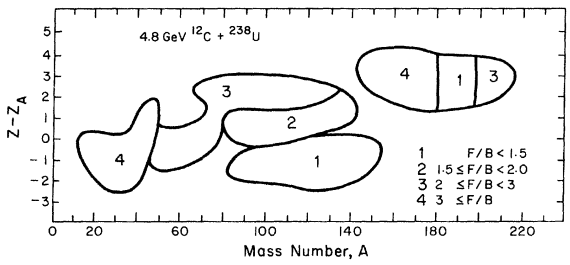

FIG. 5. A contour plot of the fragment kinetic energies $\langle E\rangle$ as deduced in the two step vector model as a function of the fragment mass number A and its position relative to the center of the valley of β stability, $Z-Z_A$, for the reaction of 4.8 GeV ^{12}C with ^{238}U.

TABLE III. Target fragment kinematic properties as deduced from the two-step vector model for 4.8 GeV $^{12}C + ^{238}U$.

Nuclide	k	N	$\langle R \rangle$ (mg/cm^2)	$\beta_{\parallel}$ ($=V_{\parallel}/c$)	P [$=AV$(MeV/c)]	$\langle E \rangle$ (MeV)
^{24}Na	0.649	1.74	16.88	0.0203	1294	42.6
^{28}Mg	0.667	1.69	15.73	0.0170	1398	42.6
^{43}K	1.004	1.32	12.29	0.0164	1833	47.9
^{44}Sc^m	1.238	1.18	9.86	0.0112	1635	36.9
^{46}Sc	1.260	1.18	11.58	0.0132	1891	47.4
^{48}Sc	1.282	1.18	9.21	0.009 01	1564	31.0
^{48}V	1.388	1.12	10.23	0.0115	1754	39.1
^{56}Mn	1.479	1.06	7.73	0.007 07	1528	25.5
^{59}Fe	1.458	1.07	8.38	0.006 46	1702	29.0
^{69}Zn^m	1.433	1.06	10.73	0.005 50	2396	51.1
^{71}As	1.304	1.07	8.92	0.007 88	2184	40.9
^{72}As	1.313	1.07	9.42	0.004 01	2302	44.7
^{74}As	1.329	1.07	8.98	0.005 91	2204	40.0
^{76}As	1.346	1.07	7.74	0.005 26	1921	29.6
^{77}Br	1.281	1.08	7.55	0.005 10	1949	30.1
^{78}As	1.363	1.07	13.74	0.006 62	3278	84.5
^{81}Rb	1.203	1.10	8.80	0.006 72	2358	41.9
^{82}Br	1.318	1.08	6.56	0.001 05	1718	22.0
^{82}Rb^m	1.210	1.10	6.47	0.004 23	1786	23.7
^{83}Rb	1.216	1.10	7.83	0.004 22	2126	33.3
^{86}Rb	1.236	1.10	7.21	0.003 17	1978	27.7
^{87}Y^m	1.129	1.13	5.79	0.004 01	1701	20.3
^{88}Zr	1.125	1.12	5.89	0.005 11	1761	21.5
^{88}Y	1.135	1.13	8.93	0.005 37	2503	43.5
^{89}Zr	1.130	1.12	7.17	0.004 74	2101	30.3
^{90}Y^m	1.146	1.13	7.80	0.005 53	2226	33.6
^{90}Nb	0.999	1.18	5.25	0.004 54	1645	54.0
^{91}Sr	1.421	1.03	10.93	0.002 42	2975	59.2
^{92}Y	1.157	1.13	7.84	0.001 07	2239	33.3
^{93}Mo^m	1.100	1.14	5.63	0.003 48	1733	19.7
^{95}Zr	1.163	1.12	9.63	0.000 94	2754	48.7
^{95}Nb	1.021	1.18	4.15	0.001 61	1360	11.9
^{95}Tc	1.012	1.18	5.60	0.005 69	1765	20.0
^{96}Nb	1.025	1.18	7.60	0.001 72	2272	32.8
^{96}Tc	1.003	1.18	6.18	0.004 18	1941	24.0
^{97}Ru	0.982	1.18	5.04	0.004 06	1681	17.8
^{97}Zr	1.174	1.12	9.74	0.001 59	2786	48.9
^{99}Mo	1.105	1.14	9.55	0.001 97	2834	49.5

TABLE III. (*Continued*).

Nuclide	k	N	$\langle R \rangle$ (mg/cm^2)	$\beta_{\parallel}$ ($=V_{\parallel}/c$)	P [$=AV$(MeV/c)]	$\langle E \rangle$ (MeV)
^{101}Rh^m	0.955	1.20	5.56	0.0046	1867	21.0
^{103}Ru	1.006	1.18	9.21	0.00228	28361	47.6
^{105}Ru	1.014	1.18	9.80	0.00090	3000	52.2
^{105}Rh	0.970	1.20	7.62	0.00383	2446	34.8
^{106}Ag^m	0.899	1.22	5.57	0.00019	1940	21.7
^{111}In	0.931	1.19	4.91	0.00389	1812	18.0
^{111}Pd^m	1.245	1.07	10.52	0.00321	3347	61.5
^{115}Cd	1.122	1.11	9.34	0.00189	3107	51.1
^{115}In^m	0.944	1.19	13.42	0.00275	4241	95.5
^{117}Sn^m	1.082	1.11	8.78	0.00380	3032	48.0
^{117}Sb	0.858	1.23	5.30	0.00187	2027	21.4
^{119}Te^m	0.703	1.34	4.81	0.00350	1932	19.2
^{120}Sb	0.867	1.23	4.37	0.00208	1739	15.4
^{121}Te	0.710	1.34	3.78	0.00346	1621	13.3
^{122}Sb	0.872	1.23	8.06	0.00205	2875	41.3
^{124}Sb	0.877	1.23	6.01	0.00018	2270	25.4
^{124}I	0.857	1.22	6.31	0.00297	2440	29.3
^{127}Sb	0.885	1.23	8.58	0.00016	3044	44.6
^{130}I	0.873	1.22	6.80	0.00179	2617	32.1
^{131}Ba	0.626	1.40	4.14	0.00341	1863	16.1
^{131}I	0.875	1.22	8.41	0.00137	3120	45.4
^{132}Te	0.728	1.34	7.15	0.00046	2665	32.9
^{132}Cs	0.780	1.27	5.59	0.00229	2295	24.3
^{132}I	0.878	1.22	5.29	0.00118	2135	21.1
^{133}I	0.881	1.22	8.78	0.00038	3240	48.1
^{135}Xe	0.948	1.18	8.20	0.00109	3087	43.1
^{135}I	0.886	1.22	8.64	0.00196	3207	46.5
^{136}Cs	0.788	1.27	6.95	0.00032	2737	33.7
^{139}Ce	0.478	1.54	2.37	0.00099	1389	8.4
^{140}Ba	0.630	1.40	5.28	0.00047	2259	22.3
^{141}Ce	0.480	1.54	7.05	0.00076	2825	34.6
^{145}Eu	0.308	1.89	2.16	0.00142	1382	8.0
^{146}Gd	0.294	1.90	1.44	0.00302	1138	5.4
^{149}Gd	0.295	1.90	2.28	0.00327	1461	8.7
^{151}Tb	0.286	1.92	1.29	0.00388	1099	4.9
^{167}Tm	0.237	2.05	1.25	0.00184	1179	5.1
^{169}Lu	0.261	1.91	2.15	0.00252	1595	9.2
^{185}Pt	0.193	2.09	1.23	0.0029	1335	5.9
^{198}Au	0.392	1.53	3.48	0.00229	2442	18.4

TABLE III. (*Continued*).

Nuclide	k	N	$\langle R\rangle$ (mg/cm^2)	$\beta_{\parallel}$ ($=V_{\parallel}/c$)	P [$=AV$(MeV/c)]	$\langle E\rangle$ (MeV)
^{198}Tl	0.227	1.90	2.47	0.00279	2020	12.5
^{209}At	0.198	1.97	2.19	0.00161	1992	11.6

most resembled similar properties for the reaction of 28 GeV protons with Au.

In this regard, it is interesting to compare our results with similar results from the interaction of high energy protons with ^{238}U. In Fig. 3, we show a comparison between the target fragment recoil properties for the reaction of 4.8 GeV ^{12}C with ^{238}U and similar measurements for the same products from the reaction of 450 MeV protons[17,18] and 3 GeV protons[18-22] with ^{238}U. One is immediately struck by the fact that the nonfission F/B values for fragments from the RHI-induced reaction generally exceed any equivalent values for the proton-induced reactions. This trend is in accord with the data for the 8.0 GeV ^{20}Ne+^{181}Ta reaction and supports the conclusion of that study[14] that at these projectile energies (4.8 GeV ^{12}C, 8.0 GeV ^{20}Ne) that limiting fragmentation has not been reached. The values of $2W(F+B)$ are similar (within certain broad limits) for the products of the heavy ion and the proton-induced reactions. To understand the meaning of this latter observation, we compared the values of $\langle P\rangle$ ($=A\langle V\rangle$) where P is the momentum of a nuclide with mass number A corresponding to the velocity V, for the neutron deficient nuclides with $(Z-Z_A)\geq 1$, where Z_A is the nonintegral Z corresponding to the center of the valley[27] of β stability for given A. $\langle P\rangle$ is the momentum imparted to the target fragments during the deexcitation step of the reaction. In examining this comparison, which is shown in Fig. 6, one may observe (within certain broad limits) a general dependence of $\langle P\rangle$ upon $\sqrt{\Delta A}$, the square root of the number of nucleons removed from the target, for the most neutron deficient species. (The solid curve represents exactly the same dependence of $\langle P\rangle$ upon $\sqrt{\Delta A}$ found[14] for the reaction of 8 GeV ^{20}Ne with ^{181}Ta. The dashed curve, which overlays the solid curve for $A=140$–200, shows the dependence of $\langle P\rangle$ upon ΔA found for several deep spallation products in proton induced reactions.[28]) This dependence would be indicative of sequential, stepwise momentum kicks being imparted to the fragment during the deexcitation phase of the reaction, in accord with the basic assumptions of the two step vector model of high energy reactions. Those nuclei resulting primarily from the fission process, have much higher values of $\langle P\rangle$ (>2750 MeV/c). The general equivalence of the $\langle P\rangle$ values for the fragments produced in proton-induced deep spallation and by the interaction of 4.8 GeV ^{12}C and 8 GeV ^{20}Ne with heavy targets would argue that the deexcitation phase of these reactions is similar. This also implies that distributions (such as certain product yield distributions) which strongly reflect the deexcitation phase will show little dependence upon projectile energy or type.

Detailed examination of the data shown in Figs. 4 and 5 shows the complexity of the target fragment kinematic properties in this reaction. In these figures, we have plotted in contour plots the values of F/B and the target fragment kinetic energy $\langle E\rangle$ as measured in a system moving with velocity $v_{\parallel}$ as a function of the displacement of the fragment atomic number Z from the valley of β stability, $Z-Z_A$. Z_A is the nonintegral Z corresponding to the center of the valley[27] of β stability for a given A. In Fig. 5, one sees evidence for the occurrence of several different processes in the reaction of 4.8 GeV ^{12}C with ^{238}U. The lightest fragments ($A<40$) are characterized by high kinetic energies and large values of F/B which is consistent with their production in a "fragmentation mechanism."[29] The heaviest fragments ($A>145$) are neutron deficient and show large values of

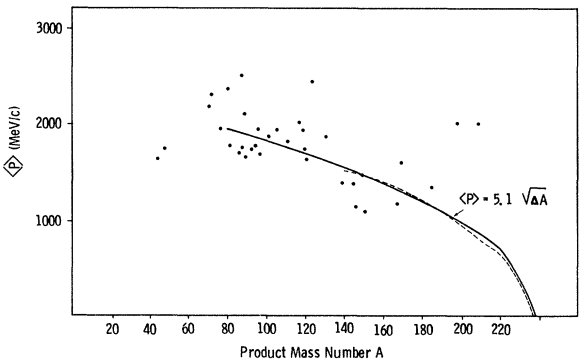

FIG. 6. A comparison of the values of $\langle p\rangle$, the momentum imparted to selected n-deficient target fragments in the reaction of 4.8 GeV ^{12}C with ^{238}U. See text for an explanation of the curves.

TABLE IV. Target fragment kinematic properties as deduced from the two step vector model for 5.0 GeV $^{20}Ne + ^{238}U$.

Nuclide	$\beta_{\parallel}$ $(=V_{\parallel}/c)$	P $[=AV(\mathrm{MeV}/c)]$	$\langle E\rangle$ (MeV)
^{24}Na	0.025	1294	42.4
^{28}Mg	0.023	1705	63.8
^{43}K	0.0049	1231	21.7
^{48}Sc	0.0083	1740	38.3
^{72}As	0.0084	1820	28.1
^{76}As	0.0050	856	5.9
^{87}Y	0.0045	2013	28.7
^{96}Nb	0.0061	2397	36.8
^{96}Tc	0.0059	2280	32.6
^{97}Zr	0.001 61	2245	31.9
^{99}Mo	0.0020	2774	47.7
^{131}I	0.000 88	2474	28.4
^{133}I	0.0016	3119	44.8
^{146}Gd	0.011	3157	41.4
^{149}Gd	0.020	3494	50.1
^{160}Er	0.0019	2388	21.5

F/B ($F/B \geq 2$) and very low fragment kinetic energies. Undoubtedly, these products are the result of deep spallation of ^{238}U nuclei. The intermediate mass products ($80 \leq A \leq 140$) are a complex mixture of fission and deep spallation products. The most n-rich products ($90 \leq A \leq 110$) are mostly fission fragments ($F/B \sim 1$, high kinetic energies). The identity of the average fissioning nucleus giving rise to these fragments is not certain. Their kinetic energies as deduced using the Northcliffe and Schilling range-energy table[26] are ~0.5 MeV/nucleon and this fact, along with their mass numbers, would suggest their formation in the fission of a species with $A \sim 210$, $Z \sim 85$. [Here we assume the fission total kinetic energy to be $Z_1Z_2e^2/1.8(A_1^{1/3}+A_2^{1/3})$]. This observation is consistent with the measurements of Remsberg *et al.*[30] who actually measured the fragment masses and energies directly in the 2.2 GeV proton induced fission of ^{238}U and deduced an average fissioning system mass of ~210. This is noteworthy because the $2W(F+B)$ values for these neutron-rich fission products from heavy ion reactions are similar to those observed in 450 MeV proton induced fission of U,[17] where much higher values of the fragment total kinetic energy were deduced because of the use of different range-energy relationships. (The authors of Ref. 17 deduced an average fissioning system of $^{234.4}U$.)

The group of fragments with $40 \leq A \leq 70$ represents an interesting class of events. Their kinetic energies are relatively high and the values of F/B are also large ($2 \leq F/B \leq 3$). One possible explanation of the origin of these events is that they represent the products of the fission of a species with $A \sim 120$–130. Their kinetic energies are completely consistent with this idea and their F/B ratios would indicate their formation in a nonperipheral collision. The other part of this scenario would be the large group of neutron-deficient products with $120 \leq A \leq 130$ which represent the nonfissioning survivors of the precursors of the $40 \leq A \leq 70$ events. Events of this character have been directly observed by Wilkins *et al.*[31] and inferred by Chang and Sugarman[32] for the reaction of high energy protons with uranium.

An alternative explanation of the origin of the $A = 40$–70 fragments suggested by the intranuclear cascade model[7] and the firestreak model[8] is that these fragments are the result of the fission of species with $A \sim 185$ that are highly excited ($E^* \geq 1000$ MeV). The resulting fission fragments evaporate copious numbers of nucleons resulting in a final fragment mass number $A \sim 40 \sim 70$.

To help our understanding of some of the empirical trends discussed above, we have compared our experimental results with two current models of relativistic heavy ion reactions, the intranuclear cascade model of Yariv and Fraenkel,[7] and a modified version of the firestreak model.[8,33] These models represent two extreme views of relativistic nuclear collisions, with the cascade model treating the projectile-target interaction as due to the uncorrelated collisions of individual particles in the projectile and target while the firestreak model assumes that all nucleons in the projectile-target overlap region interact collectively as part of the inelastic collision of two larger pieces of nuclear matter. A comparison of the results of calculations using these two models with experimental data might help to clarify the role of collective processes in energy transfer mechanism(s).

The collision of the RHI projectile with the target nucleus is treated as a two step process in the intranuclear cascade calculation, consisting of a fast step with cascading collisions of nucleons from one reaction partner inside the nucleus of the other partner and a slow statistical evaporation step deexciting the primary fragments after the fast cascading nucleons have escaped or have been captured by the primary fragments. The calculation is made using an extension of the intranuclear cascade code[34] VEGAS for proton-induced reactions which has been modified to treat two colliding nu-

clei.[7] The calculations were performed with step function density distributions for both nuclei and without refraction and reflection of the cascading particles at the nuclear boundaries. Fermi motion was included in the projectile as well as in the target nucleus. An infinite rearrangement time was assumed for the nucleus to respond to the removal of nucleons from the Fermi sea by the fast cascade. Meson production and cascades were included via the ISOBAR model.[35] The impact parameter for each collision was selected at random (with proper geometrical weighting), and the final production cross sections were integrated over impact parameter.

The deexcitation of the primary fragments from the fast cascade is calculated using a version of the Dostrovsky, Fraenkel, and Friedlander statistical model calculations[36,7] which includes fission competition. The excitation energy, mass, and atomic number of each fragment were obtained from the fast cascade calculation.

The modified firestreak model[33] is an extension of the fireball or abrasion-ablation model in which the assumption of interacting spherical nuclei with sharp surfaces making clean cuts through one another has been replaced by a more realistic assumption of interacting nuclei with diffuse surfaces due to the use of realistic nuclear density distributions.[8] The interaction between the colliding nuclei is assumed to be localized to the overlapping volume. In this region, colinear tubes of nuclear matter from the projectile and target undergo inelastic collisions with one another. (The probability of collision between the tubes is given by a transparency function based upon free nucleon-nucleon total reaction cross sections.) If the resulting kinetic energy of the collision product is less than the binding energy of the nucleus, the tube is captured by the target residue and its energy, etc., contributes to the excitation energy, linear, and angular momentum of the residue. Angular momentum is explicitly conserved in the interaction. Deexcitation of the primary products is calculated using the same formalism as the cascade model.

In Fig. 7, we show a comparison between the measured and calculated values of the longitudinal velocity $\beta_{\parallel}$ $(=v_{\parallel}/c)$ imparted to the fragment in the first step of the projectile-target interaction for the 4.8 GeV $^{12}C+^{238}U$ reaction. The measured values of $\beta_{\parallel}$ selected for use in Fig. 7 are for neutron deficient species $(Z-Z_A \geq 1)$. This selection was made to emphasize deep spallation reactions and to de-emphasize fission, i.e., to select products from collisions with significant projectile-target overlap. As one can see from examining Fig. 7, the cascade model grossly overestimates

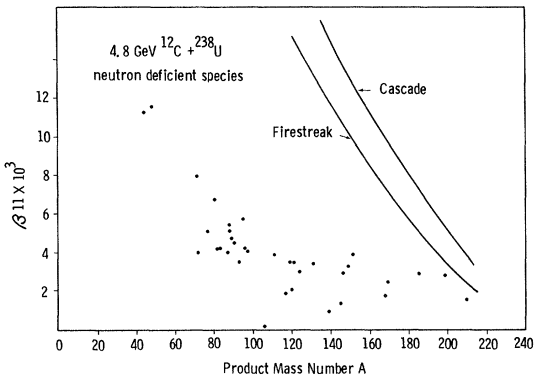

FIG. 7. A comparison of calculated and measured values of the neutron deficient target fragment longitudinal velocity component $\beta_{\parallel}$ arising from the initial target-projectile interaction for the reaction of 4.8 GeV ^{12}C with ^{238}U.

the values of $\beta_{\parallel}$ for all fragments with $A<209$, with the firestreak model predictions also in gross disagreement with the experimental data. This situation may be analogous to the overestimates of the deep spallation product momenta in proton-nucleus collisions by cascade calculations.[28] Crespo, Cumming, and Alexander[28] speculated that the primary spallation products might emit fragments such as ^{24}Na, thus reducing the spallation product momenta and providing a natural mechanism for producing the high momenta associated with these light fragments. This mechanism is not unreasonable given the calculated excitation energies (firestreak model) of the precursors of the $A=160-190$ fragments which range in energy from 380 to 595 MeV, respectively. Also, the values of β ($\approx$0.006) of the sources of the Na, etc., fragments emitted in p-U collisions[37] are supportive of this supposition because they are very similar to the calculated β values for the $A=160-190$ fragments. To help settle this question, it would be useful to measure the light fragment energies and masses in coincidence with deep spallation products from these reactions which have been identified as to energy and mass.

IV. CONCLUSIONS

What have we learned about target fragmentation in this work? The most important ideas supported by the data presented herein are as follows:

(1) The transfer of energy, momentum, etc., to the target nucleus scales with the projectile total kinetic energy for relativistic nucleus-nucleus collisions occurring with projectiles of kinetic energy 250–400 MeV/nucleon.

(2) The relativistic nucleus-nucleus collision in-

volves larger average transfer of forward momentum to the target fragments than seen in relativistic proton-induced reactions.

(3) The momentum transfer for all but the most peripheral collisions may be either substantially less than predicted by current models of RHI interactions or the primary target fragments may emit light fragments which carry away substantial amounts of momentum.

(4) There is evidence supportive of the existence of several different mechanisms in the reactions studied.

ACKNOWLEDGMENTS

This work was supported in part by the Nuclear Physics Division of the U. S. Department of Energy. We wish to thank Dr. S. B. Kaufman for allowing us to perform the 4.8 GeV ^{12}C bombardment as a parasitic experiment with his irradiation. One of us (W.D.L.) gratefully acknowledges financial support from the Lawrence Berkeley Laboratory during a portion of this work.

---

*Permanent address: Atomic Energy Research Institute, Beijing, People's Republic of China.

[1]W. Loveland, R. J. Otto, D. J. Morrissey, and G. T. Seaborg, Phys. Rev. Lett. 39, 320 (1977); see revised data in Oregon State University Report No. RLO-2227-TA35-M1, 1979, p. 24.

[2]P. L. McGaughey, W. Loveland, D. J. Morrissey, R. J. Otto, and G. T. Seaborg, Oregon State University Report No. RLO-2227-TA35-M1, 1979, p. 27; P. L. McGaughey, D. J. Morrissey, W. Loveland, and G. T. Seaborg, Lawrence Berkeley Laboratory Report No. LBL-9711, 1980, p. 92.

[3]B. V. Jacak, D. J. Morrissey, M. Rodder, and G. T. Seaborg, Lawrence Berkeley Laboratory Report No. LBL-9711, 1980, p. 94.

[4]Y. Y. Chu, E. H. Franz, G. Friedlander, and P. J. Karol, Phys. Rev. C 4, 2202 (1971).

[5]Y. Y. Chu, G. Friedlander, and L. Husain, Phys. Rev. C 15, 352 (1977).

[6]See D. J. Morrissey, W. R. Marsh, R. J. Otto, W. Loveland, and G. T. Seaborg, Phys. Rev. C 18, 1267 (1978) and references cited therein.

[7]Y. Yariv and Z. Fraenkel, Phys. Rev. C 20, 2227 (1979).

[8]W. D. Myers, Nucl. Phys. A296, 117 (1978); J. Gosset, J. I. Kapusta, and G. D. Westfall, Phys. Rev. C 18, 844 (1978).

[9]J. B. Cumming, R. W. Stoenner, and P. E. Haustein, Phys. Rev. C 14, 1554 (1976); J. B. Cumming, P. E. Haustein, R. W. Stoenner, L. Mausner, and R. A. Nausmann, *ibid.* 10, 739 (1974); J. B. Cumming, P. E. Haustein, T. J. Ruth, and G. J. Virtes, *ibid.* 17, 1632 (1978).

[10]S. B. Kaufman, E. P. Steinberg, and M. W. Weisfield, Phys. Rev. C 18, 1349 (1978).

[11]P. L. McGaughey, L. L. Nunnelley, D. J. Morrissey, W. Loveland, and G. T. Seaborg, Oregon State University Report No. RLO-2227-TA35-M1, 1979, p. 62; W. Loveland, D. J. Morrissey, R. J. Otto, and G. T. Seaborg, Lawrence Berkeley Laboratory Report No. LBL-10011 (1980).

[12]J. B. Cumming, P. E. Haustein, and H. C. Hseuh, Phys. Rev. C 18, 1372 (1978).

[13]N. T. Porile, G. D. Cole, and C. R. Rudy, Phys. Rev. C 19, 2288 (1979).

[14]W. Loveland, D. J. Morrissey, K. Aleklett, G. T. Seaborg, S. B. Kaufman, E. P. Steinberg, B. D. Wilkins, J. B. Cumming, P. E. Haustein, and H. C. Hseuh, Lawrence Berkeley Laboratory Report No. LBL-10010 (1980); Phys. Rev. C 23, 253 (1981).

[15]D. J. Morrissey, L. F. Oliveira, J. O. Rasmussen, G. T. Seaborg, Y. Yariv, and Z. Fraenkel, Phys. Rev. Lett. 43, 1179 (1979).

[16]D. J. Morrissey, D. Lee, R. J. Otto, and G. T. Seaborg, Nucl. Instrum. Methods 158, 499 (1978).

[17]N. Sugarman, H. Munzel, J. A. Panontin, K. Wielgoz, M. V. Ramaniah, G. Lange, and E. Lopez-Menchero, Phys. Rev. 143, 952 (1966); J. A. Panontin and N. Sugarman, J. Inorg. Nucl. Chem. 25, 1321 (1963); J. A. Panontin and N. T. Porile, *ibid.* 30, 2027 (1968); J. J. Hogan and N. Sugarman, Phys. Rev. 182, 1210 (1969).

[18]K. Beg and N. T. Porile, Phys. Rev. C 3, 1631 (1971).

[19]V. P. Crespo, J. M. Alexander, and E. K. Hyde, Phys. Rev. 131, 1765 (1963).

[20]O. Scheidemann and N. T. Porile, Phys. Rev. C 14, 1534 (1976).

[21]G. Friedlander, L. Friedman, B. Gordon, and L. Yaffe, Phys. Rev. 129, 1809 (1963).

[22]S. Biswas and N. T. Porile, Phys. Rev. C 20, 1467 (1979).

[23]N. T. Porile and N. Sugarman, Phys. Rev. 107, 1410 (1957).

[24]N. Sugarman, M. Campos, and K. Wielgoz, Phys. Rev. 101, 388 (1956).

[25]L. Winsberg, Nucl. Instrum. Methods 150, 465 (1978).

[26]L. C. Northcliffe and R. F. Schilling, Nucl. Data A7, 233 (1970).

[27]A. H. Wapstra and K. Bos, At. Nucl. Data Tables 19, 177 (1977).

[28]V. P. Crespo, J. B. Cumming, and J. M. Alexander, Phys. Rev. C 2, 1777 (1970).

[29]R. Wolfgang, E. W. Baker, A. A. Caretto, J. B. Cumming, G. Friedlander, and J. Hudis, Phys. Rev. 103, 394 (1956).

[30]L. P. Remsberg, F. Plasil, J. B. Cumming, and M. L. Perlman, Phys. Rev. 187, 1597 (1969).

[31]B. D. Wilkins, S. B. Kaufman, E. P. Steinberg, J. A. Urbon, and D. J. Henderson, Phys. Rev. Lett. 43, 1080 (1979).

[32]S. K. Chang and N. Sugarman, Phys. Rev. C 8, 775 (1973).

[33]The detailed extension of the firestreak model to describe target fragmentation is described in P. L.

McGaughey, D. J. Morrissey, and G. T. Seaborg, Abstract, 180th American Chemical Society National Meeting, San Francisco, 1980 (unpublished).
[34]K. Chen, Z. Fraenkel, G. Friedlander, J. R. Grover, J. M. Miller, and Y. Shimamoto, Phys. Rev. 166, 949 (1968).
[35]G. D. Harp, K. Chen, G. Friedlander, Z. Fraenkel, and J. M. Miller, Phys. Rev. C 8, 851 (1973).
[36]I. Dostrovsky, Z. Fraenkel, and G. Friedlander, Phys. Rev. 116, 683 (1959).
[37]G. D. Westfall, R. G. Sextro, A. M. Poskanzer, A. M. Zehelman, G. W. Butler, and E. K. Hyde, Phys. Rev. C 17, 1368 (1978).